arXiv:astro-ph/9909060v2 30 Nov 1999

Relativistic Winds from Compact Gamma-ray Sources: I. Radiative Acceleration in the Klein-Nishina Regime

Piero Madau[1,2] and Christopher Thompson[3]

ABSTRACT

We consider the radiative acceleration to relativistic bulk velocities of a cold, optically thin plasma which is exposed to an external source of γ-rays. The flow is driven by radiative momentum input to the gas, the accelerating force being due to Compton scattering in the relativistic Klein-Nishina limit. The bulk Lorentz factor of the plasma, Γ, derived as a function of distance from the radiating source, is compared with the corresponding result in the Thomson limit. Depending on the geometry and spectrum of the radiation field, we find that particles are accelerated to the asymptotic Lorentz factor at infinity much more rapidly in the relativistic regime; and the radiation drag is reduced as blueshifted, aberrated photons experience a decreased relativistic cross section and scatter preferentially in the forward direction. The random energy imparted to the plasma by γ-rays can be converted into bulk motion if the hot particles execute many Larmor orbits before cooling. This 'Compton afterburn' may be a supplementary source of momentum if energetic leptons are injected by pair creation, but can be neglected in the case of pure Klein-Nishina scattering. Compton drag by side-scattered radiation is shown to be more important in limiting the bulk Lorentz factor than the finite inertia of the accelerating medium. The processes discussed here may be relevant to a variety of astrophysical situations where luminous compact sources of hard X- and γ-ray photons are observed, including active galactic nuclei, galactic black hole candidates, and gamma-ray bursts.

Subject headings: gamma-rays: bursts – theory – radiation mechanisms

1. Introduction

The ejection of particles by radiation pressure has been considered many times as a possible mechanism for producing relativistic outflows from very luminous radiation sources, such as active galactic nuclei (AGNs) or galactic compact objects. In the case of an optically thin plasma, the

[1]Institute of Astronomy, Madingley Road, Cambridge CB3 0HA, UK.

[2]Institute for Theoretical Physics, University of California, Santa Barbara, CA 93106–4030.

[3]Department of Physics and Astronomy, University of North Carolina, Chapel Hill, NC 27599.

particle dynamics is dominated by the intense photon field and a flow results from the work done by the radiation force on the material.

In most previous studies it was assumed that the particles scatter photons with a cross section independent of frequency and front-to-back symmetric along the incident photon direction, such as true in the Thomson limit (Noerdlinger 1974; O'Dell 1981; Phinney 1982; Kovner 1984). Direct momentum input to the fluid at rest results when outward-directed photons are removed from the anisotropic radiation field, and then scattered away. No net momentum is carried off by the scattered photons and the material is accelerated radially. A particle moving outward near the source, however, encounters many photons nearly at right angles to its motion, more so as $v \to c$ because of aberration effects, and suffers collisional drag by them. Only mildly relativistic flows can be produced by an Eddington-limited extended source, the radiation drag actually preventing acceleration to very high particle energies (Noerdlinger 1974). In the context of AGNs, the role of Compton drag in the dynamics of relativistic jets has been the subject of many studies (e.g. Abramowicz & Piran 1980; Sikora & Wilson 1981; Phinney 1987; Melia & Königl 1989; Sikora et al. 1996).

In the past few years, the *Compton Gamma-Ray Observatory* mission has revealed the existence of some classes of objects, such as the EGRET (Fichtel et al. 1994), OSSE (McNaron-Brown et al. 1995), and COMPTEL (Bloemen et al. 1995) blazars, together with some γ-ray pulsars (Ulmer 1994), where the hard X-ray and γ-ray fluxes are a significant fraction or completely dominate the overall radiation energy budget. This is similar to what sometimes observed by the SIGMA experiment onboard of *Granat* in the case of galactic black hole candidates (Mandrou et al. 1994). The large compactnesses inferred from these data naturally lead to theoretical models in which Compton scattering in the Klein-Nishina (KN) limit (as opposed to Thomson scattering), together with photon-photon pair production may play a role in determining the thermal state and dynamics of the source. Such process may also be relevant for studies of the effects of gamma-ray bursts on their gaseous environment (their "afterglows").

In this paper we study the dynamics of a *cold* plasma embedded in the "hard" photon field of an external source. We adopt a test-particle approach, which is valid only insofar gas pressure gradients can be neglected compared to the radiative force and the material is optically thin. We consider the model problem of a fully ionized plasma where gravity is overwhelmed by radiation pressure and the distribution of particle momenta remains one-dimensional. We ignore stimulated scattering, photon absorption, and photon-electron pair production. Free-free absorption is unimportant compared to Thomson scattering if $\sigma_{ff} = 8 \times 10^{-47} n_e \, (h\nu/10^{-3} m_e c^2)^{-7/2} \, \mathrm{cm}^2 < \sigma_T$ ($h\nu \gg kT$), where n_e is the electron density. Photo-electron pair production, $\gamma e^- \to e^+ e^- e^-$ (threshold $h\nu' > 4\, m_e c^2$, where $h\nu'$ is the photon energy in the electron rest-frame) is a higher order process in the fine-structure constant, important only at large energies. (The pair production cross section is $\sim 30\%$ of the KN scattering cross section at $h\nu' = 100\, m_e c^2$, e.g. Svensson 1982.) In an accompanying paper (Thompson & Madau 1999, hereafter Paper II) we show, however, how pair creation induced by collisions between hard photons and soft side-scattered photon may increase the acceleration

rate by decreasing the inertia per particle, and by increasing the mean momentum deposited per scattering.

The plan of this paper is as follows. In § 2 we discuss the basic theory of radiative acceleration. In § 3 we present sample solutions for extended and impulsive radiation sources in the Thomson regime. Compton drag by side-scattered radiation is shown to be more effective in limiting the bulk motion than is the finite inertia of the accelerating medium. The random energy imparted to the plasma by γ-rays can be converted into bulk motion if the hot particles execute many Larmor orbits before cooling. The equation of motion in the KN limit is derived and numerically integrated in § 4 for a monoenergetic spectrum, under the assumption that the outflowing particles maintain a one-dimensional distribution of momenta, i.e. that the plasma remains 'cold' even in the presence of recoil. Blumenthal (1974) used the KN cross section to calculate the mean force due to Compton scattering on electrons with arbitrary velocity. An approximate solution to the problem of the radiative deceleration of a relativistic jet in the KN regime has been recently given by Luo & Protheroe (1999).

2. General formalism

Consider an optically thin plasma exposed to a photon source. The incident and scattered photon momenta (in units of $m_e c$) are denoted by $x\mathbf{k}$ and $x_s\mathbf{k}_s$ in the (unprimed) lab frame. Let $I_x(\mathbf{k})$ be the specific intensity of the incident radiation in the direction $\mathbf{k}$, $I(\mathbf{k}) = \int I_x(\mathbf{k})dx$. In the simplest case of a leptonic plasma composed entirely of electrons and positrons, the bulk momentum is obtained directly from the normalized phase-space density $f(\mathbf{p})$,

$$\langle \Gamma\boldsymbol{\beta}\rangle = \int \frac{\mathbf{p}}{m_e c} f(\mathbf{p}) d^3p. \tag{1}$$

Here, $\Gamma = (1-\beta^2)^{-1/2}$ as usual. This equation is easily generalized to include a hadronic component. The mean rate of momentum transfer per particle is then given by

$$\mathcal{F}_{\rm rad} = \mu c \frac{d}{dt}\langle \Gamma\boldsymbol{\beta}\rangle = -\frac{\sigma_T}{c}\int \left[\frac{x_s\mathbf{k}_s - x\mathbf{k}}{x}(1-\boldsymbol{\beta}\cdot\mathbf{k})I_x(\mathbf{k})dx d\sigma d\Omega\right] f(\mathbf{p})d^3p. \tag{2}$$

Here, μ is the mean mass per scattering charge, the angular integral is over the solid angle subtended by the source, and $d\sigma$ is the invariant differential cross section.

When the number of scattering charges is dominated by pairs, we have assumed implicitly a magnetic field strong enough to couple the pairs with the hadronic component of the plasma. The minimum flux density needed to enforce that coupling is estimated in §3.5. One must then describe the accelerating particles as a fluid, with

$$\frac{d\Gamma\beta}{dt} \rightarrow \frac{\partial \Gamma\beta}{\partial t} + c\boldsymbol{\beta}\cdot\nabla(\Gamma\beta). \tag{3}$$

In a cold plasma composed of hydrogen (of density n_p) and $e^{\pm}$ pairs (of density n_{e^+}),

$$\mu \approx m_e + m_p \left(1 + 2\frac{n_{e^+}}{n_p}\right)^{-1}. \tag{4}$$

This expression neglects the inertia of the neutralizing electron component, but not of the pairs.

The Klein-Nishina cross section for scattering of unpolarized radiation is most simply expressed in the (primed) electron rest-frame as

$$d\sigma = \frac{3}{16\pi}\sigma_T \left(\frac{x'_s}{x'}\right)^2 \left[\frac{x'}{x'_s} + \frac{x'_s}{x'} - \sin^2\chi'\right] \sin\chi' d\chi' d\phi', \tag{5}$$

e.g. Rybicki & Lightman (1979). The energy of the scattered photon is

$$x'_s = \frac{x'}{1 + x'(1 - \cos\chi')}; \tag{6}$$

in this notation, the scattering takes place through a polar angle χ' and an azimuthal angle ϕ'.

Measuring the angles θ and θ_s of the incident and scattered photon with respect to the electron velocity $\boldsymbol{\beta}$, we can write the following kinematic relations

$$\begin{aligned} x_s &= x'_s\Gamma(1 + \beta\cos\theta'_s) \\ x &= x'\Gamma(1 + \beta\cos\theta') \\ \cos\theta' &= \frac{(\cos\theta - \beta)}{(1 - \beta\cos\theta)} \\ \cos\theta'_s &= \cos\theta'\cos\chi' + \sin\theta'\sin\chi'\cos\phi'. \end{aligned} \tag{7}$$

Since the scattering cross section is independent of the azimuth ϕ', we must integrate equation (2) over two angles, χ' and θ'. The evaluation of the integral in equation (2) will be made by assuming that the radiation field is symmetric around the $\mathbf{r}$-axis, and the electrons (and positrons) will maintain a one-dimensional distribution of momenta along $\mathbf{r}$, $f(p\mathbf{n}) = f(p)\delta(\mathbf{n} - \hat{\mathbf{r}})$. Note that multiple scatterings can be safely neglected, as the singly scattered photons are beamed into a cone of half-angle $\sim 1/\Gamma$ along the electron direction of motion. Further scatterings are therefore suppressed by the $(1 - \boldsymbol{\beta}\cdot\mathbf{k}) \sim (2\Gamma^2)^{-1}$ factor in the momentum transfer equation. Single side-scattered photons will, however, be absorbed via $\gamma + \gamma \rightarrow e^+e^-$ if the compactness of the γ-ray source is high at $x \gtrsim 1$. We defer a detailed discussion of the effects of pair creation to Paper II.

3. Thomson scattering

To provide some physical insight and a framework to interpret our numerical results in the relativistic limit, we shall first discuss the acceleration of a test charge in the Thomson scattering approximation, $x' \ll 1$. In this regime, $x'_s \approx x'$ by equation (6). Thus, in the electron rest-frame,

photons of unchanged energies are scattered into an angular distribution that is forward-backward symmetric along the incident photon direction.

A particle accelerated by an external photon source will, in general, follow a curved trajectory. The problem simplifies when the source is cylindrically symmetric. From equation (2), a parcel of matter moving along the axis of symmetry with speed $\beta = c^{-1}dr/dt$ is accelerated at the rate

$$\frac{d\langle\Gamma\beta\rangle}{dt} = \frac{\sigma_T\Gamma^2}{\mu c^2}\left[(1-\beta)^2\int I(\theta)\cos\theta d\Omega - \beta\int I(\theta)(1-\cos\theta)^2 d\Omega\right]. \tag{8}$$

The first term in brackets represents the collimated flux of redshifted photons which accelerate particles radially, while the second term represents the dragging effect of the isotropic component of the radiation field.[4] The right-hand side of equation (8) vanishes for $\Gamma = \Gamma_{\rm eq}$. Particles are accelerated away from the source as long as $\Gamma < \Gamma_{\rm eq}$. If $\Gamma > \Gamma_{\rm eq}$, the force reverses, being now directed inward. This saturation of the Lorentz factor is due to the aberration into the forward hemisphere of blueshifted photons, as seen in the electron rest-frame. A particle will follow the $\Gamma = \Gamma_{\rm eq}$ equilibrium trajectory (zero-inertia limit) until, as it gets farther from the source, its acceleration is effectively limited by the large Doppler shift to the red and by the r^{-2} decline of the radiation flux.

3.1. Uniformly radiating sphere

Consider a sphere of radius R and uniform brightness I. Close to the extended source, the equilibrium Lorentz factor is

$$\Gamma_{\rm eq} \sim 3^{1/4}\,\frac{r}{R}, \tag{9}$$

no matter how high the intensity I, or whether the inertia is dominated by hadrons or leptons. In the point-source limit ($R \to 0$) the photons stream radially. For a steady flow, equation (8) reduces to

$$\frac{d\Gamma}{dr} = \Gamma^2(1-\beta)^2\widetilde{\ell}\frac{R}{r^2}. \tag{10}$$

The parameter $\widetilde{\ell}$ is the dimensionless compactness, rescaled by the inertia per scattering charge, $\widetilde{\ell} \equiv \ell(m_e/\mu) = L\sigma_T/(4\pi\mu c^3 R)$. It may be expressed as $\widetilde{\ell} = 0.5(m_p/\mu)(L/L_E)(R_S/R)$ for a source of mass M, where $L_E = 4\pi cGMm_p/\sigma_T$ is the Eddington luminosity and $R_S = 2GM/c^2$ the Schwarzschild radius. For a motion starting at radius r, the Lorentz factor attained at infinity can be obtained by solving the algebraic equation

$$2\Gamma_{\rm ps}^3(1+\beta^3) - 3\Gamma_{\rm ps} + 1 = 3\widetilde{\ell}\frac{R}{r}, \tag{11}$$

[4]This term vanishes in the case of a point-like source, $I(\mathbf{k}) = F(r)\delta(\mathbf{k}-\mathbf{r})$, where $F(r)$ is the radiative flux at radius r.

which, in the limit $\Gamma_{\rm ps} \gg 1$, yields $\Gamma_{\rm ps} \sim [3\widetilde{\ell}R/(4r)]^{1/3} = [3Lm_pR_S/(8L_E\mu r)]^{1/3}$. Effective acceleration of an e^-p plasma requires a compactness that is larger by a factor m_p/m_e than for a pure pair plasma, as a conseguence of the greater inertia per unit cross section.

Matching this solution with expression (9) yields the asymptotic bulk Lorentz factor $\Gamma_\infty \sim \widetilde{\ell}^{1/4}$ (Noerdlinger 1974). The cross-over radius beyond which the non-radial component of the radiation field causes negligible drag is $r_c \sim 0.8\widetilde{\ell}^{1/4}R$. Larger values of Γ_∞ can only be obtained if the particles are injected with relativistic bulk velocities at $r > r_c$. Bulk motion starting with $\Gamma(r) \gg \Gamma_{\rm eq}(r)$ at a distance $r < r_c$ from the source is quickly decelerated to $\Gamma \approx \Gamma_{\rm eq}$, and the excess kinetic energy converted into a collimated beam of upscattered photons.

3.2. Non-uniformly radiating disk

Infinite, Keplerian accretion disks around black holes provide an example of non-uniform radiating sources where Compton drag is most severe. The surface flux distribution as a function of equatorial radius R is given by (Shakura and Sunyaev 1973)

$$F(R) = \frac{3GM\dot{M}}{8\pi R^3}\left[1 - (3R_S/R)^{1/2}\right], \tag{12}$$

where M is now the black hole mass, and $\dot{M}$ is the accretion rate. The peak flux, $F_{\rm max} = 3GM\dot{M}/(56\pi R_{\rm max}^3)$, is reached at $R_{\rm max} = (49/12)R_S$. One can understand the essential features of the accretion disk model by approximating the flux distribution as

$$F(R) = \begin{cases} F_{\rm max}R_{\rm max}^3/R^3 & \text{if } R \geq R_{\rm max}, \\ 0 & \text{if } R < R_{\rm max}. \end{cases} \tag{13}$$

In this case the equilibrium Lorentz factor increases only as $\Gamma_{\rm eq} \sim (r/R_{\rm max})^{1/4}$ (compared to a linear increase for a spherical source). In the point-source limit, one derives $\Gamma_{\rm ps} \sim (0.75\widetilde{\ell}R_{\rm max}/r)^{1/3}$, where $\widetilde{\ell}$ is now the nominal disk compactness, $\widetilde{\ell} = 3GM\dot{M}\sigma_T/(28\pi\mu c^3R_{\rm max}^2)$. Again, by matching the two limiting solutions, the asymptotic bulk Lorentz factor is found to scale as $\Gamma_\infty \sim \widetilde{\ell}^{1/7}$ (Kovner 1984; Phinney 1987). The exact solutions for a spherical uniform source and a Keplerian accretion disk are shown in Figure 1. The latter is a much less efficient accelerator than the former because of the large photon drag associated with a radiation source extending to infinity.

3.3. Compression of the accelerating medium

The radiative force acting on an external medium induces a flow that is strongly time-dependent. One important effect of acceleration to bulk Lorentz factor Γ is the bunching of the accelerated material into a shell of thickness $\Delta r \sim r/\Gamma^2$. Let us now solve for the density of the accelerated

material. The equation of continuity of the hadronic component is

$$\frac{d(\Gamma n'_p)}{dt} + \Gamma n'_p c \frac{\partial \beta}{\partial r} = 0. \tag{14}$$

Material initially at radius r_0 reaches a radius

$$r = r_0 + c\int_{r_0/c}^{t} \beta(t')dt' = r_0 + c\int_0^{\beta} \beta' \frac{d\beta'}{f(\beta')}, \tag{15}$$

at time t (speed β). Here, $d\beta/dt = f(\beta)$. The total duration of the acceleration is

$$t - \frac{r_0}{c} = \int_0^{\beta} \frac{d\beta'}{f(\beta')}. \tag{16}$$

Eliminating r_0 from these two equations and taking $\partial/\partial r$ at constant time t, one derives $\partial\beta/\partial r = f(\beta)/c(1-\beta)$, and we have

$$\frac{1}{\Gamma n'_p}\frac{d}{dt}(\Gamma n'_p) = \frac{1}{1-\beta}\frac{d\beta}{dt}. \tag{17}$$

This integrates to

$$\frac{\Gamma n'_p}{n_{p\,0}} = \frac{1}{1-\beta} \sim 2\Gamma^2 \qquad (\Gamma \gg 1), \tag{18}$$

where $n_{p\,0}$ is the proton density in the undisturbed ambient medium.

There is a corresponding amplification of the non-radial component of a magnetic field entrained in the flow,

$$\frac{B}{B_0} = \frac{\Gamma n'_p}{n_{p\,0}} = \frac{1}{1-\beta}. \tag{19}$$

3.4. Thin photon shell

Gamma-ray sources such as blazars and gamma-ray bursts are impulsive. It is instructive, therefore, to consider a photon source that maintains a constant luminosity for a time $\Delta t \ll r/c$. This source can be visualized as a uniform shell of radius $r = ct$, thickness $c\Delta t$, and total flux $F = \int F_x dx$. We focus here on the effects of a radiation pulse and take the photons to move radially before scattering.

The compactness within the shell can be expressed directly in terms of the flux of γ-rays,

$$\ell\left(\frac{R}{r}\right) \to r\sigma_T \frac{F}{m_e c^3}, \tag{20}$$

and thence in terms of a characteristic photon optical depth,[5]

$$\tau_c \equiv \sigma_T \Delta t \frac{F}{m_e c^2}, \tag{21}$$

[5]This quantity is in fact the optical depth $\sigma_T n_\gamma(x_{\rm br}) c\Delta t$ multiplied by the frequency $x_{\rm br}$ at which the spectrum peaks.

such that $\ell(R/r) \rightarrow \tau_c(r/c\Delta t)$. Material overtaken by the photon shell at radius r, and accelerated from rest, develops a large bulk Lorentz factor when $\tau_c(m_e/\mu) \gg 1$. Integrating equation (10) in this limit yields

$$\Gamma^3 = \frac{3}{4}\widetilde{\ell}\frac{R\Delta r}{r^2} = \frac{3}{4}\,\tau_c\left(\frac{m_e}{\mu}\right)\left(\frac{\Delta r}{c\Delta t}\right) \tag{22}$$

at a radius $r + \Delta r$. As the difference between the particle speed and the speed of light decreases as $(\Delta r)^{-2/3}$, the accelerated matter will surf the photon shell over an extended range of radius, $\Delta r = \frac{2}{3}\Gamma^2 c\Delta t$. The maximum Lorentz factor is therefore

$$\Gamma_{\rm max} = \frac{\tau_c}{2}\left(\frac{m_e}{\mu}\right) \tag{23}$$

when the shell is thin enough that the acceleration length is much less than the radius, $\frac{2}{3}\Gamma^2_{\rm max}c\Delta t \ll r$ (see Figure 2). Only a limited amount of material can be accelerated to this value. Equating the kinetic energy within a volume $(4\pi/3)r^3$ with the energy of the photon shell implies a very high pre-existing optical depth to Compton scattering, $\tau_T = \sigma_T\rho r/m_p \sim 6$. Since our calculation of $\Gamma_{\rm max}$ is valid only for small τ_T, the ambient density at radius r is bounded above by

$$\rho < \frac{\mu}{\sigma_T r} = 2\times10^{-9}\left(\frac{\tau_c}{300}\right)^{-2}\left(\frac{\Delta t}{10\ {\rm s}}\right)^{-1}\left(\frac{\mu}{m_p}\right)^{3}\left(\frac{3r}{2\Gamma^2_{\rm max}c\Delta t}\right)^{-1}\ \ {\rm g\ cm^{-3}}. \tag{24}$$

Note the strong dependence on μ. We will show is Paper II that, even if the ambient medium is composed of a hadronic plasma initially (as is expected in most cosmological gamma-ray burst models), the mean mass per scattering charge will be rapidly reduced to $\mu \sim m_e$ by pair creation.

Sidescattered photons will provide additional drag that reduces Γ below the value given in equation (23). As the photon shell propagates ahead of an accelerating parcel of matter, it generates an isotropic radiation field of photon density

$$\frac{n_\gamma^{\rm iso}}{n_\gamma} \sim n_s\sigma_T\frac{r^2}{\widetilde{\ell}R}, \tag{25}$$

where $n_s \equiv n_p + 2n_{e^+}$ is the density of scattering charges in the ambient medium at rest, and $r^2/\widetilde{\ell}R$ is the lengthscale over which isotropic scattering occurs (before the scattering medium gets accelerated to relativistic velocities). The net effect is to introduce a second, negative term into equation (10), which becomes

$$\frac{d\Gamma}{dr} = \left(\frac{1}{4\Gamma^2} - \frac{4}{3}\Gamma^2 n_s\sigma_T\frac{r^2}{\widetilde{\ell}R}\right)\frac{\widetilde{\ell}R}{r^2} \tag{26}$$

at large Γ. Acceleration up to Lorentz factor $\Gamma_{\rm max}$ is then possible only if the ambient density is lower than

$$\rho < \frac{3\tau_c}{16\Gamma^4_{\rm max}}\,\frac{m_e}{\sigma_T c\Delta t}. \tag{27}$$

This bound is stronger by a factor $\sim \Gamma^{-1}$ than equation (24): *in the Thomson scattering regime, the bulk Lorentz factor is actually limited by side-scattered radiation.* This conclusion changes when

the photon source is very hard, because side-scattered photons are immediately consumed by pair creation (Paper II). A compact source of γ-rays always tends, in this sense, to maintain a radial photon distribution.

3.5. Compton afterburn

It is well known that a hot (relativistic) plasma in an anisotropic radiation field feels a much larger radiation pressure than a cold (non-relativistic) gas of the same inertial mass (O'Dell 1981), and tends to drive itself away from the radiation source with momentum derived largely from the anisotropic loss of its own internal energy. This "Compton rocket" is, however, ineffective at generating bulk relativistic motion from internal random kinetic energy, as it is always accompanied by catastrophic Compton cooling (Phinney 1982). Nonetheless, by integrating the momentum equation in the limiting case of a cold plasma we are actually underestimating its bulk Lorentz factor: the gas will be continuously heated by the hard radiation field itself, hot particles will radiate most of their energy in the direction of the radiation source, and part of the energy of relativistic random motion will be converted into bulk motion. We term this supplementary source of momentum the 'Compton afterburn'. The afterburn can be largely neglected in the case of pure KN scattering without pair creation (§ 4.1). (In Paper II we will consider a situation in which relativistic e^+e^- pairs are injected into an anisotropic photon beam by collisions between side-scattered photons and the main beam – thereby inducing a net force on the plasma as they Compton cool.) Nonetheless, we discuss it here for completeness.

The afterburn is strongest when the radiative force on the relativistic, cooling particles is coupled to the rest of the fluid through a background magnetic field. Above a critical flux density which we estimate, this allows the colder particles to dominate the inertia of the flow, and the momentum gained by Compton scattering to be more effectively absorbed rather than being radiated away. The afterburn is easiest to analyze when the period of a cyclotron orbit is much shorter than the Compton cooling time. Then the linear momentum imparted to one charge is effectively shared with the others before the charge loses its excess energy in the bulk frame. We also assume that the acceleration time is long compared with the Compton cooling time, so that the proportion of energetic particles is small. This is the case when the energetic charges are continually regenerated, e.g., by pair creation. Finally, we assume that the magnetic field is non-radial (as is appropriate to the rest frame of a plasma that has been accelerated to relativistic speed). We divide the velocity of the charge into components $\beta_{e\perp}$ and $\beta_{e\parallel}$ perpendicular and parallel to $\mathbf{B}$, and denote by η the angle between the cyclotron motion and the radial direction.

The charge is immersed in a collimated photon beam of energy flux

$$F_\Gamma = \frac{1}{2\Gamma^2} F = \frac{1}{2\Gamma^2} \int F_x dx \qquad (\Gamma \gg 1) \tag{28}$$

in the boosted frame of the bulk flow. It feels a radial force (O'Dell 1981)

$$\frac{d}{dt}\left(\frac{p_r}{m_e c}\right) = \frac{\sigma_T F_\Gamma}{m_e c^2}(1-\beta_{e\perp}\cos\eta)\Big[\gamma_e^2(1-\beta_{e\perp}\cos\eta)(-\beta_{e\perp}\cos\eta)+1\Big]. \tag{29}$$

The net radial momentum imparted to the cooling charge is obtained by averaging over a cyclotron orbit, $\eta \to \eta + 2\pi$,

$$\left\langle \frac{d}{dt}\left(\frac{p_r}{m_e c}\right)\right\rangle = \frac{\sigma_T F_\Gamma}{m_e c^2}\Big(\gamma_e^2\beta_{e\perp}^2+1\Big). \tag{30}$$

At the same time, the net energy lost to Compton cooling is

$$\left\langle \frac{d\gamma_e}{dt}\right\rangle = -\frac{\sigma_T F_\Gamma}{m_e c^2}\gamma_e^2\left(\frac{1}{2}\beta_{e\perp}^2+\beta_e^2\right). \tag{31}$$

When the energetic charges are created with $\beta_{e\,\parallel}=0$ (e.g., pair creation between a hard radial photon and a soft side-scattered photon), the cooling rate is $d\gamma_e/dt = -(3\sigma_T F_\Gamma/2m_e c^2)\,\gamma_e^2\beta_e^2$ and the radial momentum gained as the particle cools is

$$\frac{d(p_r/m_e c)}{d\gamma_e} = -\frac{2\gamma_e^2}{3(\gamma_e^2-1)}. \tag{32}$$

To leading order in γ_e,

$$\frac{p_r}{m_e c} \simeq \frac{2}{3}\gamma_e. \tag{33}$$

In this case, the source of energy for the charge is external to the accelerating medium. The charge carries an excess lab-frame momentum $(2\Gamma)\gamma_e m_e c$, which is supplemented by (33) to yield a total $\frac{5}{3}(2\Gamma)\gamma_e m_e c$ (in the limit $\gamma_e \gg 1$).

These expressions change slightly when the energetic charges are distributed isotropically, and reduce to those found by O'Dell (1981). The rate of Compton cooling is $d\gamma_e/dt = -(4\sigma_T F_\Gamma/3m_e c^2)$ $\gamma_e^2\beta_e^2$, as usual, and

$$\frac{d(p_r/m_e c)}{d\gamma_e} = -\frac{\gamma_e^2+\frac{1}{2}}{2(\gamma_e^2-1)}. \tag{34}$$

The *net* radial momentum acquired is

$$\frac{p_r}{m_e c} \simeq \frac{1}{2}\gamma_e, \tag{35}$$

only 3/10 of the value obtained for charges that are created moving parallel to the photon beam.

These calculations assume that a high energy particle will execute many cyclotron orbits before Compton cooling. Let us check when this assumption is valid. The rest frame magnetic flux density is related to the initial (non-radial) field before acceleration by

$$B' = \frac{B_0}{\Gamma(1-\beta)} \simeq 2\Gamma\, B_0 \tag{36}$$

(eq. 19). Each fresh (radially-moving) particle has a rest-frame energy $\gamma_e m_e c^2 \simeq E/2\Gamma$, and so it takes a time

$$t'_{\rm cyc} = \frac{\gamma_e m_e c}{eB'} \simeq \frac{1}{4\Gamma^2}\,\frac{E}{eB_0 c} \tag{37}$$

to complete one radian of a Larmor orbit. The Compton cooling time is

$$t'_{\rm cool} = \frac{2m_e c^2}{3\gamma_e \sigma_T F_\Gamma}. \tag{38}$$

The energy flux in a thin photon shell is related to the characteristic optical depth τ_c (eq. 21) through $\sigma_T F/m_e c^2 = \tau_c/\Delta t$, and so the ratio of these two timescales is

$$\frac{t'_{\rm cyc}}{t'_{\rm cool}} \sim \frac{3}{32\Gamma^5}\tau_c \left(\frac{E}{m_e c^2}\right)^2 \left(\frac{m_e c}{eB_0 \Delta t}\right) = 2\times 10^{-4}\,\frac{\tau_c}{\Gamma^5}\left(\frac{E}{m_e c^2}\right)^2 \left(\frac{B_0}{3\times 10^{-6}\ {\rm G}}\right)^{-1}\left(\frac{\Delta t}{10\ {\rm s}}\right)^{-1}. \tag{39}$$

The compression of the accelerating medium has a related consequence: the mean energy $\langle\gamma_e\rangle$ of the scattering charges in the bulk frame increases due to adiabatic heating, at a rate $\langle\gamma_e\rangle^{-1}(d\langle\gamma_e\rangle/dt) = \frac{1}{3}n'^{-1}(dn'/dt) = \frac{1}{3}\Gamma^{-1}(d\Gamma/dt)$ in the lab frame. A balance between compressional heating and Compton cooling results in an equilibrium energy $\langle\gamma_e\rangle$ that is only mildly relativistic. As a result, we will assume that the heating process has isotropized the momenta of the pairs in the bulk frame:

$$\frac{1}{\langle\gamma_e\rangle}\frac{d\langle\gamma_e\rangle}{dt} = \frac{1}{3\Gamma}\frac{d\Gamma}{dt} - \frac{4}{3}\frac{\langle\gamma_e\rangle}{t^0_{\rm cool}}. \tag{40}$$

The reference (lab-frame) cooling time is $t^0_{\rm cool} = m_e c^2/\sigma_T \Gamma F_\Gamma \simeq (\Gamma x_{\rm br}/2\tau_c)\Delta t$. The acceleration rate is decreased by a factor $\sim \langle\gamma_e\rangle^{-1}$ from the value calculated above for a cold plasma:

$$t_{\rm accel} = \frac{\Gamma}{d\Gamma/dt} \simeq \langle\gamma_e\rangle\, t^0_{\rm accel}. \tag{41}$$

¿From equation (10), we have

$$\frac{t^0_{\rm cool}}{t^0_{\rm accel}} = \frac{1}{2\Gamma^2}\frac{m_e}{\mu} \tag{42}$$

at $\Gamma \gg 1$. Even in the case of a pair-loaded plasma ($\mu \simeq m_e$), one sees that energetic particles cool faster than the bulk flow accelerates. The same conclusion holds for scattering in the Klein-Nishina regime (§ 4), but not when pair creation drives the acceleration (Paper II).

4. Klein-Nishina regime: monoenergetic spectrum

When $x' \gtrsim 1$ recoil can no longer be neglected. In the general case, the integral over the scattering angle χ' of the Compton force on particles moving along the **r**-axis,

$$\frac{d}{dt}\langle\Gamma\beta\rangle = -\frac{1}{\mu c^2}\int \frac{x_s\cos\theta_s - x\cos\theta}{x}\,(1-\beta\cos\theta) I_x dx d\sigma d\Omega, \tag{43}$$

can be performed analitically by making the variable change $\chi' \rightarrow x'_s$, and integrating the resulting polynomial in x'_s. The mean rate of momentum transfer can then be written as

$$\frac{d}{dt}\langle\Gamma\beta\rangle = \frac{\sigma_T}{\mu c^2}\int(1-\beta\cos\theta)K(x')\left[\cos\theta + \frac{\Gamma(\cos\theta-\beta)}{x(1-\beta\cos\theta)}\right]I_x dx d\Omega, \tag{44}$$

where $K(x') \equiv \int x'_s(1-\cos\chi')d\sigma/\sigma_T$ can be evaluated in closed form,

$$K(x') = \frac{3}{4x'^2}\left[\frac{x'^2-2x'-3}{2x'}\ln(1+2x') + \frac{-10x'^4+51x'^3+93x'^2+51x'+9}{3(1+2x')^3}\right] \tag{45}$$

(cf. Blumenthal 1974). This function has limiting behavior

$$K(x') \approx \frac{3}{8x'}[\ln(2x') - 5/6 + ...] \tag{46}$$

for $x' \gg 1$, and

$$K(x') \approx x'(1-21x'/5 + ...) \tag{47}$$

for $x' \ll 1$. The first term in the last expansion, when substituted back into equation (44) in the limit $x' \ll 1$, reproduces the standard Thomson results of equation (8) (for $\mu = m_e$). [6]

Figure 3 shows the integrand function in equation (44), $P \equiv (1-\beta\cos\theta)K(x')\{\cos\theta+\Gamma(\cos\theta-\beta)/[x(1-\beta\cos\theta)]\}$, versus incident photon angle for different photon energies and particle valocities. The aberration effect of outward-directed photons into the forward hemisphere (as observed in the electron rest-frame) is clearly seen, together with the reduced radiative force as γ-ray photons are preferentially scattered in the forward direction. In the Thomson limit, photons at angles $\cos\theta < \beta$ with respect to the direction of motion are seen in the rest-frame of the electron as blueshifted and inward directed, and work to decelerate the flow ($P < 0$). The same criterion does not apply in Klein-Nishina, as blueshifted, aberrated photons experience a decreased relativistic cross section and are scattered less efficiently. When $\beta = 0.8$, for example, the rate of momentum transfer becomes negative at angles $\cos\theta < 0.71, 0.35$, and 0.13 for photons with energy $x = 0.5, 3$, and 10, respectively.

The complexity of the KN cross section foils analytic calculations of the particle trajectories. We have numerically integrated equation (44) with the Runge-Kutta method assuming a monoenergetic photon spectrum. The equilibrium Lorentz factor as a function of distance from a radiating

[6]The force on a e^-p plasma at rest relative to a point-source of mass M and monoenergetic flux $F(r)$ is, from equation (44), $d\langle\Gamma\beta\rangle/dt = (\sigma_T/m_p c^2)F(r)K(x)(1+x)/x$. The Eddington luminosity for which this force just balances the gravitational attraction at all radii r is then given by

$$L_E = \frac{4\pi c G M m_p}{\sigma_T}\left[\frac{x}{K(x)(1+x)}\right],$$

where the term in parenthesis (equal to 2.4, 5.9, and 11.8 for $x = 0.5, 3$, and 10, respectively) is the relativistic correction factor to the classical expression in the Thomson limit (Blumenthal 1974).

sphere and a disk is shown in Figure 4 for different energies of the incoming photons. While in the Thomson limit the radiation drag imposes a linear relation between $\Gamma_{\rm eq}$ and distance r from a spherical source, in Klein-Nishina the importance of this braking force is reduced: the zero-inertia limit is reached then at higher particle velocities. The net momentum transfer in each interaction with a γ-ray photon is significantly lower, however, and it is actually more difficult (i.e. larger compactnesses are needed) for an electron to approach the zero-inertia limit (Figure 4). In Figure 5 the asymptotic Lorentz factor at infinity is depicted as a function of source compactness for different incoming photon energies. A comparison with the Thomson limit shows that γ-ray photons with $x = 10$ (say) are significantly more efficient at accelerating particles only for compactness $\widetilde{\ell} \gtrsim 200$, and more so in the extended disk case (i.e. when the isotropic radiation field is larger) than for a spherical source. In the general case, the detailed dynamics of an the plasma will depend on the energy spectrum of the incoming radiation (Paper II).

The KN reduction of the photon drag can be easily quantified in the extreme case of a jet moving with relativistic speed towards a point-source of γ-rays. From equation (44) we derive

$$\frac{d}{dt}\langle\Gamma\beta\rangle = -\frac{\sigma_T F(r)}{\mu c^2}\,(1+\beta^2)\Gamma^2\left[\frac{K(x')}{\Gamma^2(1+\beta)}\left(1+\frac{\Gamma}{x}\right)\right], \tag{48}$$

where $x' = x\Gamma(1+\beta)$. The term in parenthesis, equal to 0.094, 0.016, and 0.006 for $\Gamma = 2$ and $x = 0.5, 3$, and 10, respectively, is the relativistic correction to the braking force in scattering Thomson.

4.1. Compton heating

Together with momentum, energy will be transferred from the radiation field to the gas at a rate

$$\begin{aligned}\left\langle\frac{dE}{dt}\right\rangle &= -\frac{1}{\mu c^2}\int\frac{x_s - x}{x}\,(1-\beta\cos\theta)I_x dx d\sigma d\Omega \\ &= \frac{\sigma_T}{\mu c^2}\int(1-\beta\cos\theta)K(x')\left[1+\frac{\Gamma\beta(\cos\theta-\beta)}{x(1-\beta\cos\theta)}\right]I_x dx d\Omega. \end{aligned}\tag{49}$$

Equations (44) and (49) assume that all the particles in a small volume element of gas (that moves with bulk Lorentz factor Γ) are at rest with respect to that volume element. Because of recoil in each collision, however, the plasma will be Compton heated (hence $\langle dE/dt\rangle \neq d\Gamma/dt$ in eq. 49) to relativistic temperatures, and in general these equations should be integrated over the appropriate distribution function. [7] The integral can can solved numerically for a momentum distribution that is isotropic in the electron rest-frame (e.g. a relativistic Maxwellian) provided the relaxation time of the plasma is short compared with the dynamical time.

[7] In the absence of any other cooling or heating mechanisms, a thermal gas will be driven towards the Compton temperature $T_C = m_e c^2\langle x\rangle/(4k)$. For a power-law spectrum with energy indices $\alpha = 0$ and -1.5 below and above the break frequency $x_{\rm br} = 1$ (characteristic of gamma-ray bursts), one derives $\langle x\rangle = 0.74$ and $T_C = 1.1\times10^9$ K.

In the case of a cold plasma at rest in an *isotropic* photon bath, the Compton heating rate per unit volume can be written, from equation (49) with $x' = x$,

$$H = 4\pi n_s \sigma_T \int \left[\frac{K(x)}{x}\right] x I_x dx, \tag{50}$$

where the term $K(x)/x$ (equal to 0.28, 0.04, and 0.008 for $x = 0.5, 3$, and 10, respectively) is the KN reduction factor to the classical Thomson formula. It has been recently pointed out that Compton heating of electrons by hard X-ray background photons may provide a significant energy source for the intergalactic medium (Madau & Efstathiou 1999). It is crucial in the cosmological context to use equation (50) rather the Thomson limit, as relativistic corrections become increasingly more important at early times when the peak in spectral power of the X-ray background (observed today at ~ 30 keV) is blueshifted to higher energies.

It is also worth noting that the efficiency of the Compton afterburn should be further diminished in the KN regime, as the decreased relativistic cross section reduces the anisotropy (between highly scattering electrons moving towards the source and those, less scattering, moving away) that ultimately drives the effect (Phinney 1982; see also Renaud & Henry 1998). The afterburn may be a supplementary source of momentum if the energetic particles are injected by an external energy source, and if they execute many Larmor orbits while cooling (§3.5). However, in the present context (in which the particles are assumed cold before scattering) only a small increase in the bulk momentum will result from the afterburn effect. Even if we suppose that *all* the energy transferred from the radiation field to the gas is actually converted into bulk motion, and integrate equation (49) with $\langle dE/dt \rangle = d\Gamma/dt$, we get asymptotic Lorentz factors that are at most ten percent higher than those computed from the momentum equation.

We have benefited from stimulating discussions with G. Blumenthal, G. Ghisellini, and M. Rees. Support for this work was provided by NSF through grant PHY94-07194 (P. M.), and by the Sloan foundation (C. T.).

REFERENCES

Abramowicz, M. A., & Piran, T. 1980, ApJ, 241, L7

Bloemen, H., et al. 1995, A&A, 293, L1

Blumenthal, G. R. 1974, ApJ, 188, 121

Fichtel, C. E., et al. 1994, ApJS, 94, 551

Kovner, I. 1984, A&A, 141, 341

Luo, Q., & Protheroe, R. J. 1999, MNRAS, in press (astro-ph/9901223)

Madau, P., & Efstathiou, G. 1999, ApJ, 517, L9

Mandrou, P., et al. 1994, ApJS, 92, 343

Melia, F., & Königl, A. 1989, ApJ, 340, 162

Noerdlinger, P. D. 1974, ApJ, 192, 529

O'Dell, S. L. 1981, ApJ, 243, L147

Phinney, E. S. 1982, MNRAS, 198, 1109

Phinney, E. S. 1987, in Superluminal Radio Sources, ed. J. A. Zensus & T. J. Pearson (Cambridge: Cambridge Univ. Press), 301

Renaud, N., & Henri, G. 1998, MNRAS, 300, 1047

Rybicki, G. B., & Lightman, A. P. 1979, Radiative Processes in Astrophysics (New York: Wiley)

Shakura, N. I., & Sunyaev, R. A. 1973, A&A, 24, 337

Sikora, M., Sol, H., Begelman, M. C., & Madejski, G. M. 1996, MNRAS, 280, 781

Sikora, M., & Wilson, D. 1981, MNRAS, 197, 529

Svensson, R. 1982, ApJ, 258, 335

Thompson, C., & Madau, P. 1999, submitted to the ApJ (Paper II)

Ulmer, M. P. 1994, ApJS, 90, 789

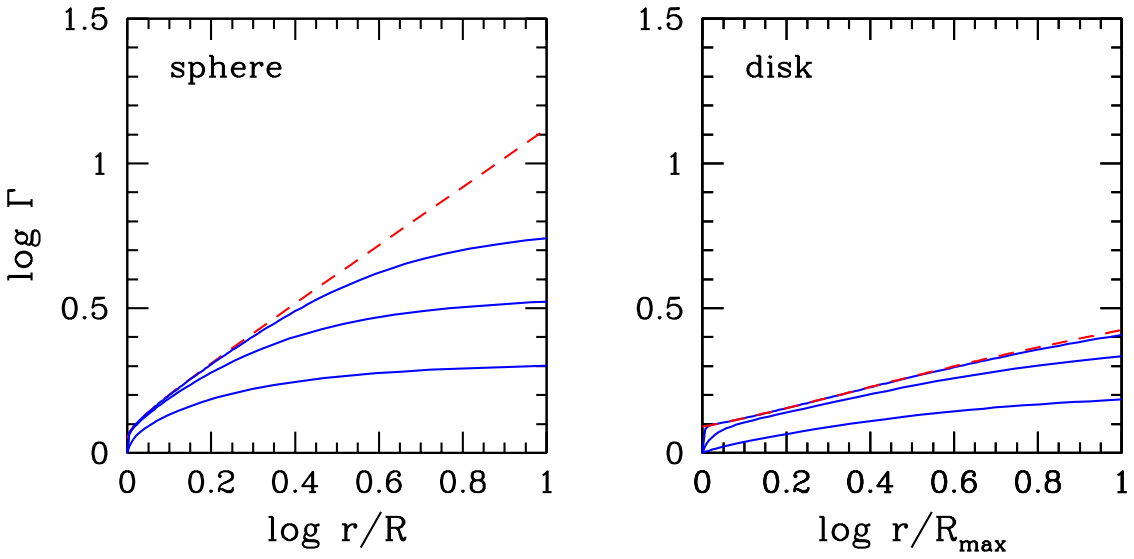

Fig. 1.— *Left:* Bulk Lorentz factor of a test particle as a function of distance r from a uniformly radiating sphere of radius R and compactness $\widetilde{\ell}$. The equation of motion has been integrated in the Thomson regime assuming the particle is initially at rest. From top to bottom: $\widetilde{\ell} = 1000, 100, 10$ (*solid lines*). *Dashed line*: Zero-inertia limit. *Right:* Same but for an infinite, Keplerian accretion disk (see text for details).

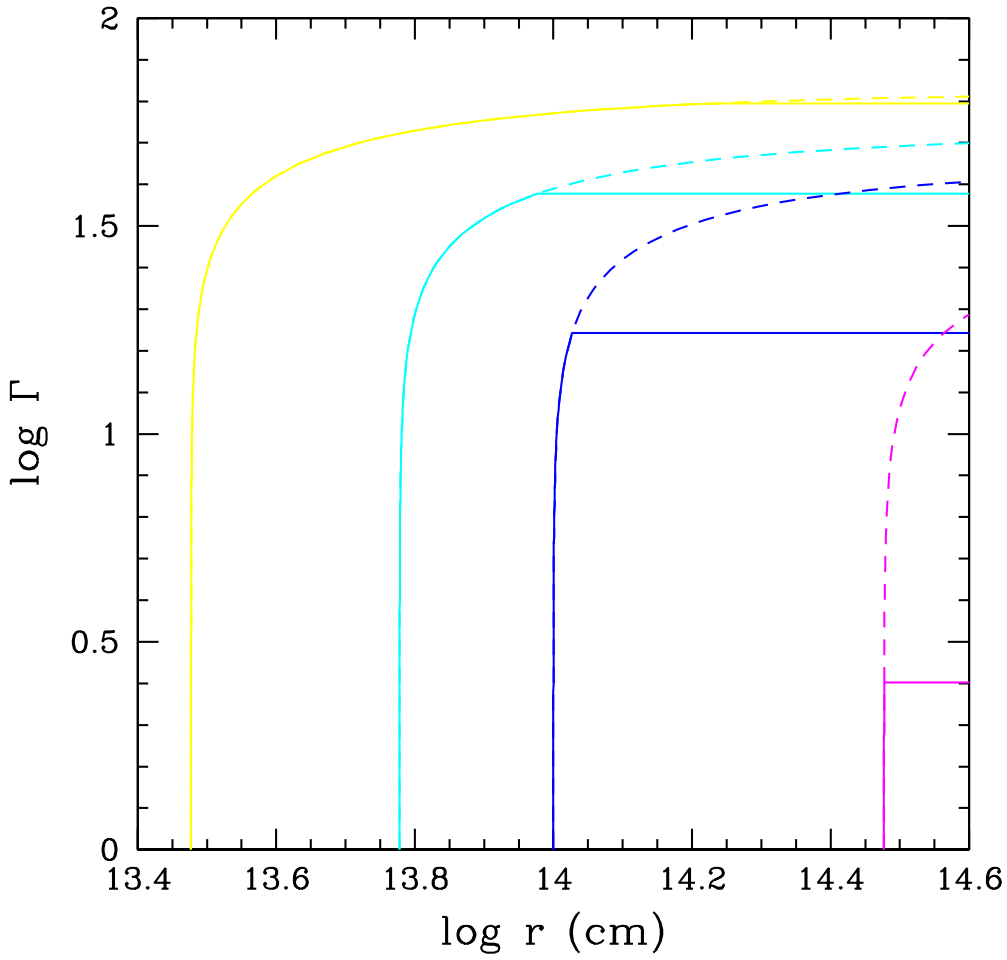

Fig. 2.— Bulk Lorentz factor of a test particle ($\mu = m_p$) as a function of distance r (in cm) from a point-like source of luminosity 10^{52} ergs s^{-1}. The equation of motion has been integrated in the Thomson regime assuming the particle to be initially at rest. *Solid curves*: radiation pulse of duration 1 sec. The radiative force vanishes when the photon shell moves past the particle. *Dashed curves*: steady source.

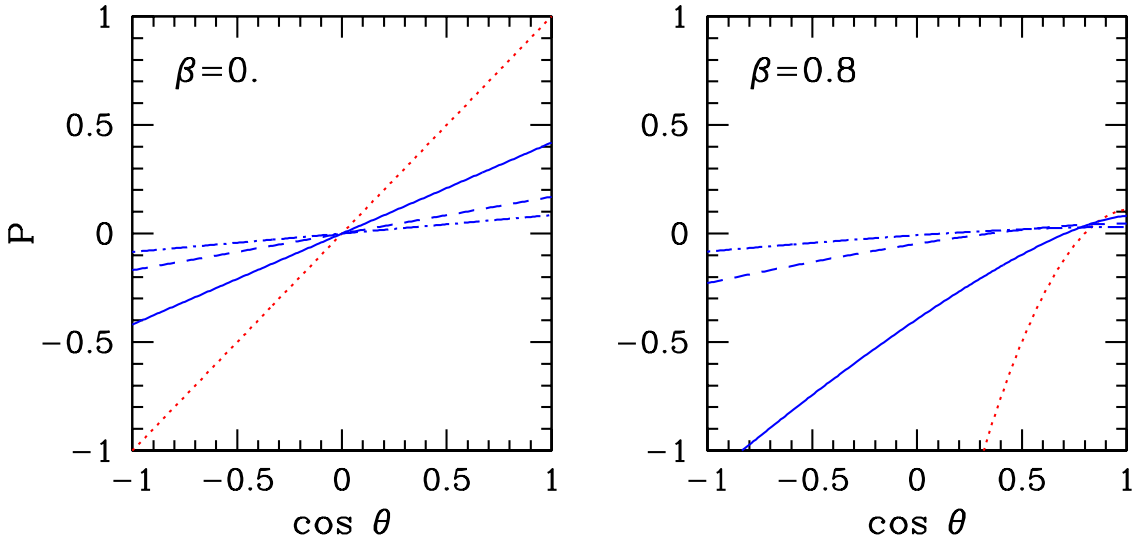

Fig. 3.— Specific rate of momentum transfer per unit solid angle (see eq. 44), $P \equiv (1-\beta\cos\theta)K(x')\{\cos\theta+\Gamma(\cos\theta-\beta)/[x(1-\beta\cos\theta)]\}$, versus incident photon angle for different photon energies x (in units of m_ec^2) and particle valocities β (in units of c). *Solid line:* $x = 0.5$. *Dashed line:* $x = 3$. *Dash-dotted line:* $x = 10$. *Dotted line:* Thomson limit.

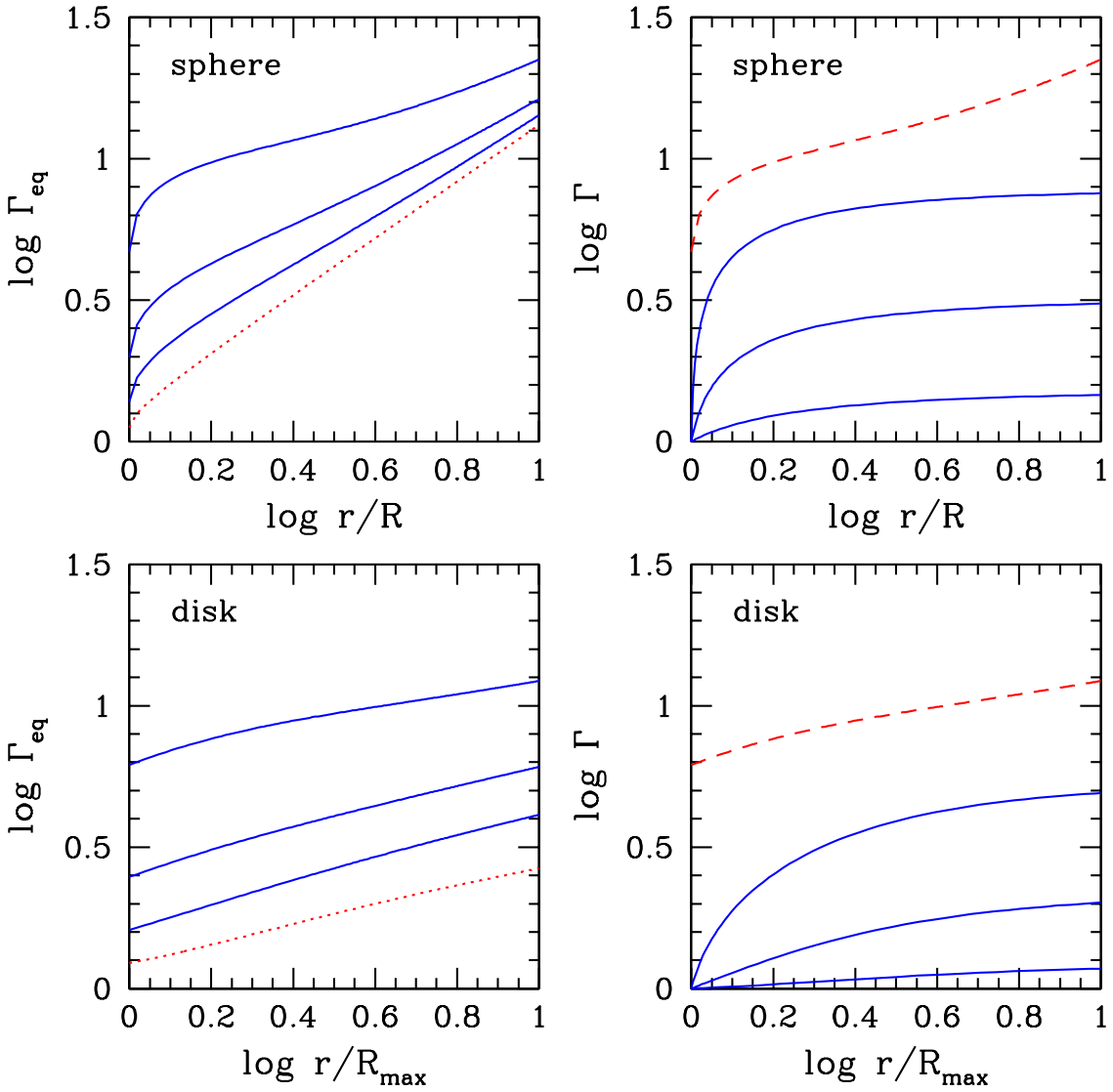

Fig. 4.— *Top left:* Equilibrium Lorentz factor (zero-inertia limit) of a test particle as a function of distance r from a uniformly radiating sphere of radius R. The photon spectrum is monoenergetic and the equation of motion has been integrated in the Klein-Nishina regime. *Solid lines:* Values obtained for different energies of the incoming photons: $x = 10, 3, 1$ (from top to bottom). *Dotted line:* Thomson limit. *Top right:* Bulk Lorentz factor as a function of distance. The equation of motion has been integrated using the relativistic cross section and assuming the particle to be initially at rest. The radiation spectrum is monoenergetic with photon energy $x = 10$. From top to bottom: $\widetilde{\ell} = 1000, 100, 10$ (*solid lines*). *Dashed line*: Zero-inertia limit. Note how, in the relativistic limit, the particle velocity saturates to its asymptotic value at infinity much closer to the radiation source than in the Thomson regime (cf. Fig. 1). *Bottom:* Same for a Keplerian accretion disk.

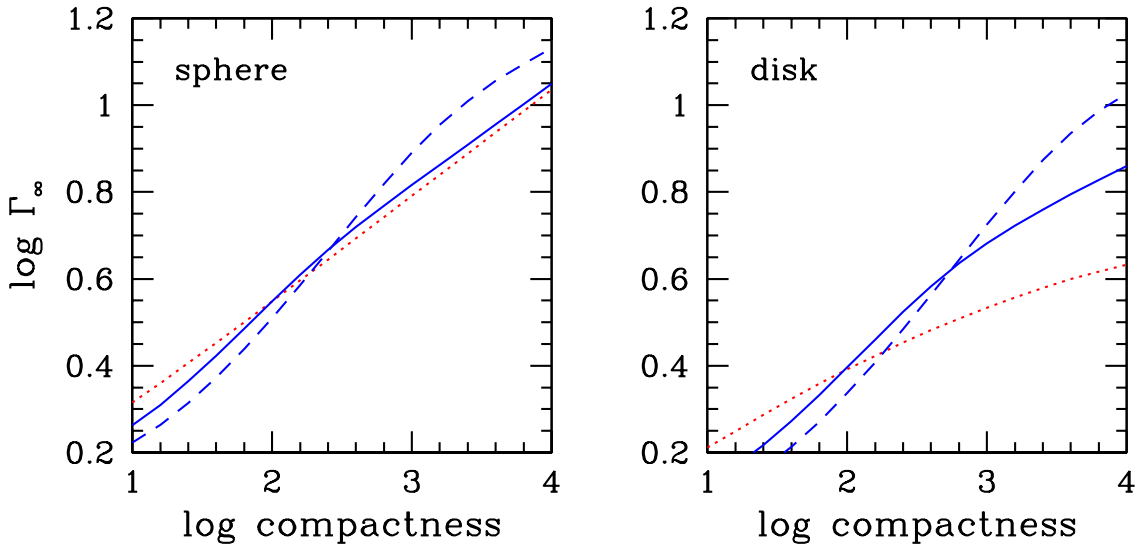

Fig. 5.— Asymptotic Lorentz factor at infinity as a function of compactness for a particle initially at rest. *Solid line:* KN cross section, incoming photon energy $x = 3$. *Dashed line:* Same for $x = 10$. *Dotted line:* Thomson limit. *Left:* Uniformly radiating sphere. *Right:* Keplerian accretion disk.